Radio-Frequency Coils in Implantable Devices: Misalignment Analysis and Design Procedure

MANI SOMA, MEMBER, IEEE, DOUGLAS C. GALBRAITH, MEMBER, IEEE, AND ROBERT L. WHITE, FELLOW, IEEE

Abstract—**Radio-frequency (RF) coils are used extensively in the design of implantable devices for transdermal power and data transmission. The practical issues of coil misalignments and configurations have not been investigated, and this paper presents a detailed theoretical analysis of misalignment effects in RF coil systems, including lateral and angular misalignments. Formulas are derived for the mutual inductance and, whenever possible, simplified upper bounds and lower bounds of the coupling coefficient are provided. A design procedure is established to maximize coil coupling for a given configuration, and a companion paper [1] discusses a circuit design technique to reduce the effects of misalignment on transmission efficiency.**

INTRODUCTION

THE rapid advances of microelectronic applications in biomedical engineering have resulted in an increasing number of implantable devices for stimulation of muscles or nerve tissues. To avoid the possibility of infection by wires piercing the skin and the undesirable replacement of an implanted power source, these devices usually receive power and stimulation data via an inductively coupled radio-frequency coil system. The primary coil is outside the body and driven by an external transmitter circuit. The secondary coil is implanted with the device and connected to the receiver circuit. In implantable devices such as cochlear or visual prostheses, the coils are separated by a layer of skin and tissues, usually less than 1 cm thick. Due to anatomical requirements, the coils are frequently misaligned, thus reducing the coupling efficiency. The effects of misalignment on efficiency have never been investigated in detail both from the geometrical standpoint and from the circuit design standpoint. A design procedure was given by Ko [2] for the perfectly aligned case of two solenoid coils, and Flack [3] provides computer-derived graphs for the lateral misalignment case. Hochmair [4] also considers the lateral misalignment case and reduces the mutual inductance double integral to a single integral, which is then solved by numerical integration. Almost all designs still rely on the experimental work by Terman [5], trial-and-error techniques for each particular case, or numerical evaluations.

Manuscript received July 15, 1985. This work was supported by the National Institutes of Health under Contract N01-NS-5-2306.

M. Soma is with the Department of Electrical Engineering, University of Washington, Seattle, WA 98195.

D. C. Galbraith is with Actel, Inc., Sunnyvale, CA 94087

R. L. White is with Stanford Electronics Laboratories, Stanford University, Stanford, CA 94305.

IEEE Log Number 8612606.

Considering the importance of radio-frequency (RF) coils in implantable devices, it is desirable to establish a formal design procedure which takes into account all misalignment cases and provides realistic estimates of the coil coupling efficiency. This paper presents a detailed theoretical investigation of the lateral and angular misalignment effects, and the companion paper [1] discusses a circuit design technique to stabilize the link efficiency and gain in the presence of misalignment.

Since the theoretical development of the mutual inductance in arbitrary coil configurations is complicated due to the lack of symmetry, we will proceed in the following order.

1) The textbook case of perfect alignment (Fig. 1) will be considered first to establish some mathematical conventions and to be used in comparison to nonideal cases.

2) The lateral misalignment case (Fig. 2), where two coils are in parallel planes but their centers are displaced by a distance Δ, will be studied in conjunction with some mathematical techniques to approximate the coupling coefficient.

3) The angular misalignment case (Fig. 4), where the planes of the coils are tilted to form an angle α and the axis of one coil passes through the center of the other coil, will be studied using essentially the same approximating techniques.

4) The general case (Fig. 6), where both lateral and angular misalignments are present, will be considered last based on the results developed in previous sections.

For simplicity, we will assume the case of one-turn coils first, and will consider later the effects of number of turns. The coil sizes and misalignment parameters are specified in Table I with reference to the Neuman's formula for mutual inductance [6].

$$M = \frac{\mu_0}{4\pi} \oint\oint \frac{dl_1 \cdot dl_2}{r_{12}} \tag{1}$$

PERFECT ALIGNMENT CASE

The perfect alignment case is treated in detail by textbooks (see for example [6]), and referring to Fig. 1, the mutual inductance is given by

$$M_i = \mu_0 \sqrt{ab} \left\{ \left(\frac{2}{k} - k \right) K(k) - \frac{2}{k} E(k) \right\} \tag{2}$$

0018-9294/87/0400-0276$01.00

TABLE I
COIL AND CONFIGURATION PARAMETERS

Parameter	Meaning
a, b	Coil radii
d	Coil spacing
Δ	Lateral misalignment
α	Angular misalignment
M_i	Mutual inductance (ideal)
M_L	Mutual inductance (lateral case)
M_A	Mutual inductance (angular case)
M	Mutual inductance (general case)
μ_0	Free-space permeability ($4\pi \times 10^{-7}$ H/m)

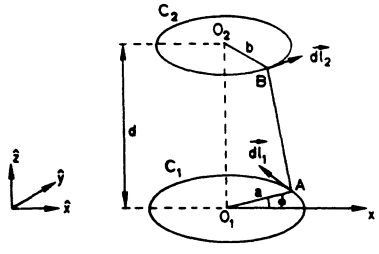

Fig. 1. Ideal perfectly aligned coil configuration.

where

$$k \equiv \left(\frac{4ab}{(a+b)^2 + d^2}\right)^{1/2} \tag{3}$$

and $K(k)$ and $E(k)$ are the complete elliptic integrals of the first and second kind, respectively.

The bracketed expression in (2) appears quite often in the following analysis, and will be denoted by

$$G(r) \equiv \left(\frac{2}{r} - r\right) K(r) - \frac{2}{r} E(r). \tag{4}$$

Equation (2) is now written as

$$M_i = \mu_0 \sqrt{ab}\, G(k). \tag{5}$$

This exact expression will be used as the basis for comparing the mutual inductances in the nonideal cases to follow.

LATERAL MISALIGNMENT CASE

The configuration to be considered is shown in Fig. 2. Despite the loss of perfect cylindrical symmetry, reflective symmetry across the plane perpendicular to the coils and passing through O_1O_2 is preserved. The factors in Neuman's formula become more involved but can still be evaluated easily.

$$dl_1 = ad\phi \tag{6a}$$

$$dl_2 = bd\theta \tag{6b}$$

$$r_{12} = \sqrt{a^2 + b^2 + d^2 + \Delta^2 - 2\Delta a \cos\theta + 2\Delta b \cos\phi - 2ab\cos(\phi - \theta)}. \tag{6c}$$

By introducing

$$b_L \equiv \sqrt{b^2 + \Delta^2 + 2\Delta b \cos\phi} \tag{7a}$$

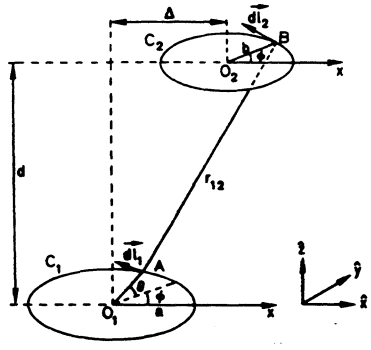

Fig. 2. Lateral coil configuration.

$$\tan\beta \equiv \frac{\Delta \sin\phi}{b + \Delta\cos\phi} \tag{7b}$$

the expression for r_{12} can be simplified to

$$r_{12} = \sqrt{a^2 + b_L^2 + d^2 - 2ab_L \cos(\theta + \beta)}. \tag{8}$$

The mutual inductance integral takes the form

$$M_L = \frac{\mu_0}{4\pi} ab \oint d\phi \oint \frac{\cos\theta\, d\theta}{r_{12}}. \tag{9}$$

Integrating over θ yields

$$M_L = \frac{\mu_0 ab}{2\pi} \oint \frac{\cos\beta}{\sqrt{ab_L}} G(r)\, d\phi \tag{10}$$

where

$$r \equiv \left(4a \frac{b_L}{(a + b_L)^2 + d^2}\right)^{1/2} \tag{11}$$

and the function G is defined by (4).

The simple appearance of the integrand in (10) is deceptive since the ϕ dependence is concealed in the parameters β, b_L, and r. When $\Delta = 0$ (perfect alignment), these parameters are constant with respect to ϕ, and M_L reduces to M_i. When $\Delta \neq 0$, it is impossible to integrate exactly. Flack [3] resorted to numerical integration to solve this problem, a technique which, although acceptable, tends to be costly in repeated computer runs during the design phase when the coil sizes have not been specified or when optimization with respect to Δ is attempted. Another solution is to derive the upper and lower bounds for M_L, which are very valuable during the design phase since these bounds determine the theoretical maximum and minimum coupling for any coil system. Also of interest is some approximate value for M_L, since this value is required for circuit design and system efficiency calculations. It will be shown that the upper and lower bounds are rather easy to calculate, and the approximate formulas are both computationally efficient and accurate within 10 percent of the exact value.

The bounds can be derived by noting that

a) b_L (7a) is monotonically increasing in cos ϕ. This result can be proved by differentiating b_L with respect to cos ϕ, which yields a positive derivative.

b) the function

$$f(\phi) = \frac{\cos \beta}{\sqrt{ab_L}} \tag{12}$$

is monotonically decreasing in cos ϕ. This statement can be verified by studying the derivative of $f(\phi)$ with respect to cos ϕ and by assuming that the misalignment Δ is smaller than the radius b, which is true in almost all implantable coil systems. The minimum value of $f(\phi)$ is obtained by setting cos $\phi = +1$, and the maximum value of $f(\phi)$ is obtained by setting cos $\phi = -1$ in (12).

c) the function $G(r)$ is monotonically increasing in cos ϕ for most realistic cases where the misalignment Δ is of the order of the distance d, and of course is also less than b. Again, this statement can be verified by checking the sign of the derivative of $G(r)$ with respect to cos ϕ. The minimum and maximum values of $G(r)$ can be obtained by setting cos $\phi = -1$ and cos $\phi = +1$, respectively.

Replacing $f(\phi)$ and $G(r)$ by their minimum values (which are now independent of ϕ) over the integration range from 0 to 2π, (10) is easily integrated to yield the lower bound of the mutual inductance.

$$M_L(\min) = \frac{\mu_0 ab}{\sqrt{a(b + \Delta)}} G(r_{\min}) \tag{13}$$

where

$$r_{\min} \equiv \left(\frac{4a(b - \Delta)}{(a + b - \Delta)^2 + d^2} \right)^{1/2} \tag{14}$$

Note that we have assumed $\Delta < b$ in the above formulas, which is the usual case. For misalignments larger than the radius b, the evaluation of the bounds is more complicated but the procedure is identical to that followed here.

Repeating the procedure by replacing $f(\phi)$ and $G(r)$ by their maximum values over the integration range, the upper bound of the mutual inductance is

$$M_L(\max) = \frac{\mu_0 ab}{\sqrt{a(b - \Delta)}} G(r_{\max}) \tag{15}$$

where

$$r_{\max} \equiv \left(\frac{4a(b + \Delta)}{(a + b + \Delta)^2 + d^2} \right)^{1/2} \tag{16}$$

It should be noted that the bounds computed by (13) and (15) are extremely conservative since we have separately replaced each function in the integrand by its extremal values without considering the integrand as a whole. To approximate M_L more closely without further cumbersome analysis, we use the maximum value of $G(r)$ and the minimum value of $f(\phi)$, which yields

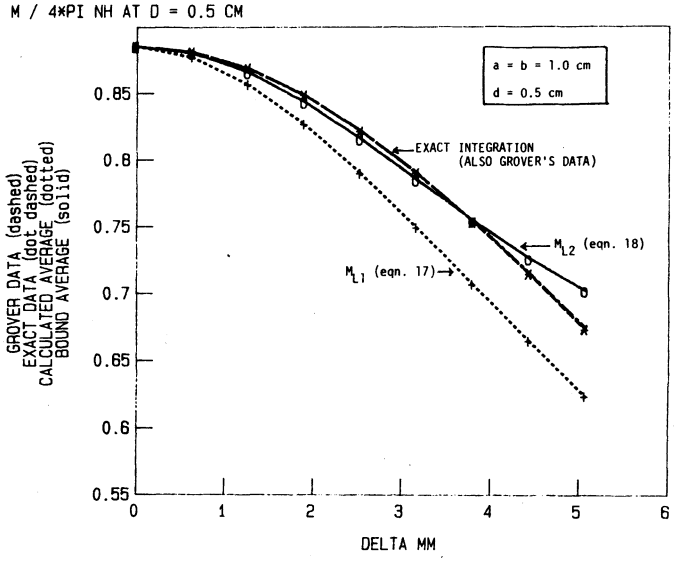

Fig. 3. Mutual inductance under lateral misalignments (normalized by 4π nH).

$$M_{L1} = \frac{\mu_0 ab}{\sqrt{a(b + \Delta)}} G(r_{\max}). \tag{17}$$

This average value, normalized by the constant 4π nH, is plotted in Fig. 3 for a representative coil set used in cochlear prostheses [7] characterized by

$$a = 1.0 \text{ cm}, \quad b = 1.0 \text{ cm},$$
$$d = 0.5 \text{ cm}, \quad \Delta \text{ up to } 0.5 \text{ cm}.$$

Also plotted in Fig. 3 are the exact values computed by numerical integration, and the arithmetic average of the maximum and minimum bounds given by (13) and (15). We note the following.

1) The average value (17) always underestimates the mutual inductance except in the ideal case where it is exact.

2) The average value deviates less than 10 percent from the exact values even at large misalignments.

3) The arithmetic average of the bounds

$$M_{L2} = \frac{M_L(\max) + M_L(\min)}{2} \tag{18}$$

is an excellent approximation of the mutual inductance and tends to overestimate at very large misalignments. The overestimation error is usually small.

Thus, both (17) and (18) can be used to approximate M_L within 10 percent of the exact values. The advantage of these equations over the usual numerical integration of the mutual inductance integral is that misalignment sensitivity and optimal coil sizes can be studied based on the closed-form derivatives of M_L with respect to a, b, d, Δ, and other partial derivatives. The interaction in the parameter set (a, b, d, Δ) is more evident. For example, by studying the derivatives of M_L with respect to d and Δ, we reach the expected conclusion that at large coil distances, relatively large lateral misalignments have no significant effects on the mutual inductance.

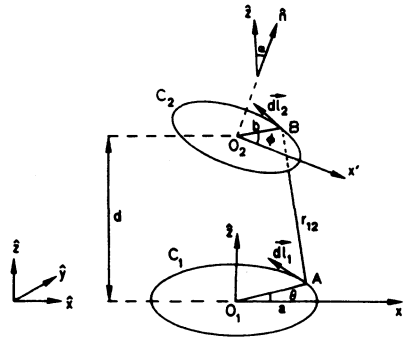

Fig. 4. Angular coil configuration.

Angular Misalignment Case

The configuration to be studied is shown in Fig. 4. Note that symmetry still exists across the plane perpendicular to coil 1 and passing through the coil centers. The line elements dl_1 and dl_2, and the distance r_{12} are evaluated by geometrical methods

$$\vec{dl}_1 = a(-\sin\theta\hat{x} + \cos\theta\hat{y})\,d\theta \tag{19a}$$

$$\vec{dl}_2 = b(-\sin\phi\cos\alpha\hat{x} + \cos\phi\hat{y} + \sin\phi\sin\alpha\hat{z})\,d\phi \tag{19b}$$

$$r_{12} = \sqrt{a^2 + b^2 + d^2 - 2ab(\cos\theta\cos\phi\cos\alpha + \sin\theta\sin\phi) - 2bd\cos\phi\sin\alpha}. \tag{19c}$$

The mutual inductance integral is

$$M_A = \frac{\mu_0 ab}{4\pi}\oint\oint \frac{\sin\theta\sin\phi\cos\alpha + \cos\theta\cos\phi}{r_{12}}\,d\theta\,d\phi. \tag{20}$$

The numerator can be manipulated by adding and subtracting $\cos\theta/\cos\phi$, which yields

$$M_A = \frac{\mu_0 ab}{4\pi}\oint d\phi \left(\oint \frac{\tan\phi\,[\sin\theta\cos\phi\cos\alpha - \cos\theta\sin\phi]}{r_{12}}\,d\theta + \oint \frac{\cos\theta}{r_{12}\cos\phi}\,d\theta\right). \tag{21}$$

The integration over θ in the first double integral yields zero, thus

$$M_A = \frac{\mu_0 ab}{4\pi}\oint d\phi\oint \frac{\cos\theta}{r_{12}\cos\phi}\,d\theta. \tag{22}$$

By introducing

$$\tan\lambda \equiv \frac{\sin\phi}{\cos\phi\cos\alpha} \tag{23}$$

the mutual inductance integral can be simplified to

$$M_A = \frac{\mu_0 ab}{4\pi}\oint d\phi\oint\left(\frac{(\cos\theta/\cos\phi)\,d\theta}{a^2 + b^2 + d^2 - 2bd\cos\phi\sin\alpha - 2ab\dfrac{\cos\phi\cos\alpha\cos(\theta - \lambda)}{\cos\lambda}}\right)^{1/2}. \tag{24}$$

Note that λ is independent of θ. The integral over θ can be evaluated in closed form to give a combination of the complete elliptic integrals similar to the above two cases.

$$M_A = \frac{\mu_0\sqrt{ab}}{\pi\sqrt{\cos\alpha}}\int_0^{\pi}\left(\frac{\cos\lambda}{\cos\phi}\right)^{3/2} G(r)\,d\phi \tag{25}$$

where

$$r \equiv \left(\frac{4ab\cos\phi\cos\alpha/\cos\lambda}{a^2 + b^2 + d^2 - 2bd\cos\phi\sin\alpha + 2ab\cos\phi\cos\alpha/\cos\lambda}\right)^{1/2} \tag{26}$$

and the function G is defined by (4).

We first note that in the perfect alignment case $\alpha = 0$, the mutual inductance M_A reduces to the ideal expression for M_i (5). Under angular misalignment, (25) cannot be integrated exactly, and by the same methods used in the lateral misalignment case, the bounds and average values for M_A can be evaluated. The bounds are again too conservative to be usable, but two approximations are reasonably close to the exact values computed by numerical integration. The first approximation involves replacing r in (25) by the average of its extremal values over the integration range, and the second approximation assumes realistic misalignments less than 25°. The approximate formulas for M_A are given by

$$M_{A1} = \frac{\mu_0\sqrt{ab}}{\sqrt{\cos\alpha}}\,G(\bar{r}) \tag{27}$$

$$M_{A2} = \frac{M_i}{\sqrt{\cos\alpha}} \tag{28}$$

where M_i is the mutual inductance in the ideal case ($\alpha = 0$), G is the function defined by (4), and

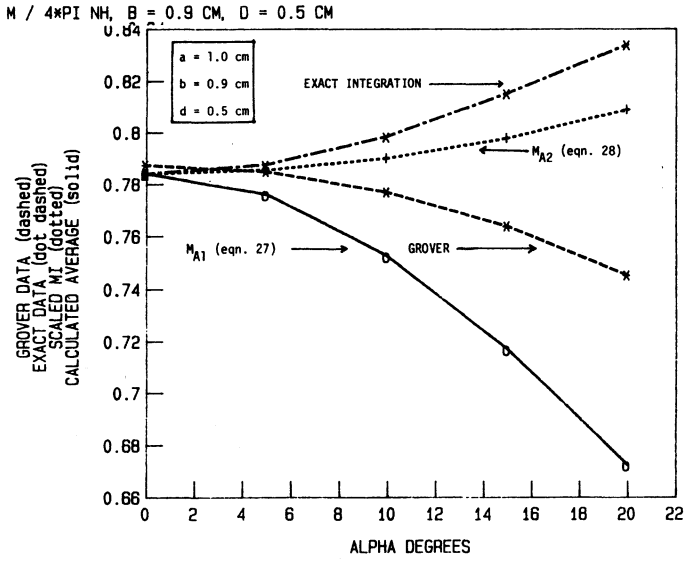

Fig. 5. Mutual inductance under angular misalignments (normalized by 4π nH).

$$\bar{r} \equiv \frac{r_{\max} + r_{\min}}{2} \tag{29}$$

$$r_{\max} = \left(\frac{4ab \cos \alpha}{a^2 + b^2 + d^2 - 2bd \sin \alpha + 2ab \cos \alpha} \right)^{1/2} \tag{30a}$$

$$r_{\min} = \left(\frac{4ab \cos \alpha}{a^2 + b^2 + d^2 + 2bd \sin \alpha + 2ab \cos \alpha} \right)^{1/2} \tag{30b}$$

These formulas for a coil set characterized by

$$a = 1.0 \text{ cm}, \quad b = 0.9 \text{ cm},$$
$$d = 0.5 \text{ cm}, \quad \alpha \text{ up to } 20°$$

are plotted in Fig. 5.

Note that we have used $b = 0.9$ cm to accommodate Grover's estimated data [8] (his tables do not cover the case $a/b = 1$), and that all inductance values are normalized by 4π nH. Fig. 5 shows the following.

1) The approximation based on averaging the values of r (27) always underestimates the numerically computed values, but the error is still less than 20 percent for angles up to 20°.

2) The approximation based on the ideal value scaled by cos α (28) is easily computed and is correct within 3 percent of the exact values even for large angles.

3) Grover's data are significantly poorer than (28) in estimating the mutual inductance under angular misalignments.

We note the interesting behavior of M_A as an increasing function of the misalignment angle, which accounts for most of the errors in the first approximation (27) and in Grover's data. This behavior is easily explained and was pointed out by Hochmair [4]: the tilting of the receiver coil brings half of the coil closer to the perimeter of the transmitting coil, and since the magnetic field is maximized at the coil perimeter, we expect increasing coupling, which overcompensates some losses due to the larger distance between the transmitting coil and the other half of the receiving coil. In the angular misalignment configuration, the distance between the coil centers is no longer a good indicator of the mutual inductance, and designers should also study the smallest and largest distances between the coils to get a realistic measure.

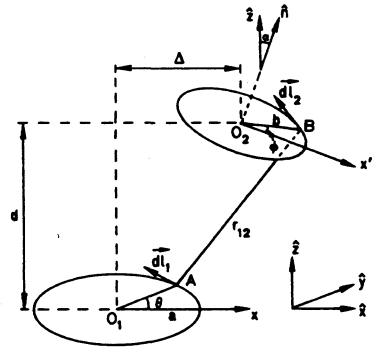

Fig. 6. General coil configuration.

General Case

The general case, illustrated in Fig. 6, incorporates both lateral and angular misalignments. The same analysis procedure may be used to compute the mutual inductance M as follows.

1) Write the expressions for $\vec{dl}_1$, $\vec{dl}_2$, and r_{12} based on geometrical considerations.

2) Simplify the double integral by trigonometric manipulations. It is possible to integrate exactly one of the two integrals just as shown above.

3) The remaining integral cannot be integrated in closed form, but upper and lower bounds can be computed by studying the behavior of the integrand over the integration range.

A faster, and probably less accurate, procedure to derive the expressions for M is to note that under angular misalignment alone, a good approximation (28) is to scale the ideal value by $\cos \alpha^{-1/2}$. Under the assumption that there is no strong interaction between the lateral misalignment and the angular misalignment, it is reasonable to estimate the general mutual inductance by applying the same scale factor to the values derived for the case of lateral misalignment. In other words, the mutual inductance may be approximated by either of the two following expressions.

$$M_1 = \frac{M_{L1}}{\sqrt{\cos \alpha}} \tag{31}$$

$$M_2 = \frac{M_{L2}}{\sqrt{\cos \alpha}} \tag{32}$$

where M_{L1} and M_{L2} are given by (17) and (18).

These approximate formulas for the case

$$a = 1.0 \text{ cm}, \quad b = 1.0 \text{ cm},$$
$$d = 0.5 \text{ cm}, \quad \alpha = 15°$$

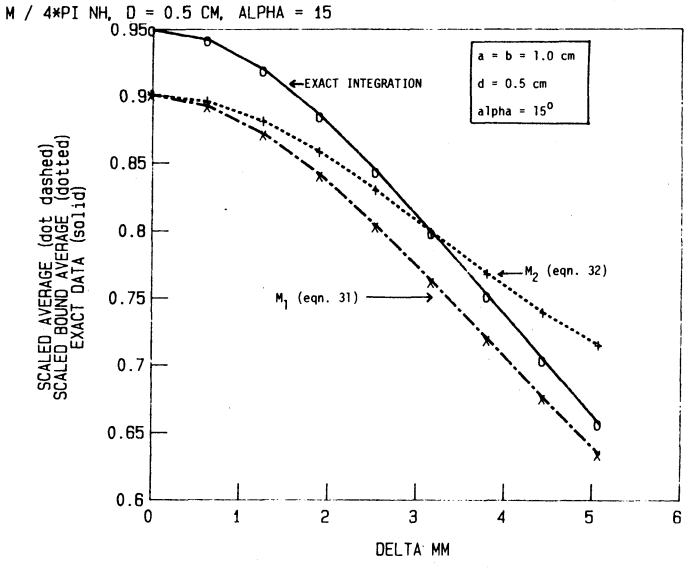

Fig. 7. General mutual inductance (normalized by 4π nH).

are plotted in Fig. 7 together with the values computed by numerical integration. The normalization factor is 4π nH, and there are no data available from Grover's tables since they do not cover the general case of both angular and lateral misalignments. We note that both approximations are excellent at large lateral displacements, and underestimate the correct value by less than 6 percent at small lateral displacements. These discrepancies can be explained as follows.

1) At small lateral misalignments, the angular effect dominates. The mutual inductance increases as explained above; the underestimation error can be traced to the error committed by using the scale factor $\cos \alpha^{-1/2}$ in the angular case. Note that the 5 percent error in Fig. 7 is comparable to the 3 percent error in Fig. 5 at the point $\alpha = 15°$.

2) At large lateral misalignments, the lateral effect dominates. The approximations in (31) and (32) thus should come closer to the correct value, which is the case in Fig. 7. The error due to either approximation is again less than 10 percent. At large Δ, M_{L1} underestimates and M_{L2} overestimates the correct value, which is expected under lateral misalignment.

The assumption that there is no strong interaction between two misalignment effects, which was made to arrive at (31) and (32), is thus well justified.

Since misalignment is inevitable in RF coil systems used in prostheses, (31) and (32) are essential in estimating the mutual inductance and in choosing coil sizes given the expected ranges of lateral and angular misalignments. The coil design process is iterative and it is important that the mutual inductance be estimated quickly and efficiently without laborious calculations. With this consideration in mind, we note that the approximated values in (31) and (32) are easy to compute compared to numerical integration procedures used by all other investigators. While the presence of the elliptic integrals might suggest some numerical integration, they can actually be evaluated by very efficient iterative procedures published by the ACM [9]. The formulas presented herein are always easier to evaluate than double integrals, especially in the general case of both misalignments, where even the integrand itself becomes so mathematically complicated as to obfuscate the effects of coil parameters on the mutual inductance.

Practical Coils

The practical coils used in implantable devices fall into two categories.

1) Disk coils or pancake coils: the longitudinal thickness of these coils is small compared to the radial thickness and coil radius. Each coil is essentially a flat spiral.

2) Solenoid coils: the longitudinal thickness of these coils is appreciably larger and the radial thickness is appreciably smaller than a comparable pancake coil. Each turn of the coil has approximately the same radius.

It is immediately apparent that the mutual inductance calculation of practical coils has to take into account two effects: the number of turns, and the coil shape. A straightforward application of Neuman's formula is mathematically intractable since neither the line elements nor the limits of integration can be written in any simple forms. Two general approaches to the solution of this problem are the following.

1) Number of Turns: Instead of calculating the mutual inductance, it is simpler to calculate the coupling coefficient k since

$$k = \frac{M}{\sqrt{L_1 L_2}}. \tag{33}$$

For coils of n_1 and n_2 turns, the mutual inductance is scaled by $n_1 n_2$, the self-inductance of the transmitter L_1 is scaled by n_1^2, and the self-inductance of the receiver L_2 is scaled by n_2^2. Thus, the effect of the number of turns cancels out in the calculation of the coupling coefficient. In other words, we can use the formulas developed above for the one-turn case to calculate the mutual inductance, and from the textbook formulas for the self-inductance of one-turn coils, compute the coupling coefficient.

The question posed by this procedure is the values of the coil parameters to be used in the above formulas. For example, each pancake coil has two radii: which one should be used? How can an average radius be computed? For solenoid coils, there is the question of coil distance. These questions are related to the coil shape, which are discussed below.

2) Coil Shape: The usual method of taking into account coil shapes is to define a set of average parameters, e.g., average radii, average distances, etc., compute the coupling coefficient based on this average set, and multiply the result by some empirically determined factors. Numerous works have been published regarding these methods ([8] and [5]); Grover's tables [8] in particular provide a wealth of parameters for all practical coil shapes and sizes. Any of these methods may be used in conjunction with the above formulas as follows.

a) Define the average dimensions for the coils. For ex-

ample, the arithmetic mean of the radii of a pancake coil can be used as the average radius, or the distance between the center planes of solenoid coils can be defined as the average coil distance.

b) Compute the mutual inductance for one-turn coils, using the formulas derived in this paper.

c) Compute the self-inductances for one-turn coils, using shape correction factors published in [8] and [5] if necessary.

d) Compute the coupling coefficient, using (33) and shape correction factors associated with mutual inductance calculations.

While this method might seem an uneasy alliance between analytical results and empirical correction factors, the exact analysis of the general case of mutual inductance of arbitrary coils under misalignments is still an open problem. Even for the special solenoid cases treated by [4] assuming only lateral misalignments, we note that most computations in that work were done for planar circular coils, i.e., ideal solenoids with zero thickness. Under the same assumptions, the results presented herein are accurate (within 10 percent) and computationally efficient in estimating the coupling coefficient.

Design Procedure

Based on the above analysis, the design procedure for implantable coil systems to take into account geometrical misalignments is the following.

1) Determine the coil parameters based on system consideration. For example, the receiver coil radius is limited by the implant site, or the ratio of the numbers of turns is set by gain calculations.

2) Determine the nominal and worst-case angular and lateral misalignments based on anatomical considerations of the implant site and other system criteria (e.g., effects of the packaging of the receiver on the coil alignment).

3) Determine an average parameter set for one-turn coils and use the formulas above to calculate the coupling coefficient. Shape correction factors may be incorporated as mentioned.

4) If the coupling coefficient does not meet other design goals (system bandwidth, gain, etc.), iterate this procedure. Note that thanks to the analytical forms of the mutual inductance equations, the sensitivity of the coupling coefficient with respect to a particular parameter can be quickly and efficiently determined.

Conclusion

This paper presents a cohesive analytical derivation of the mutual inductance for coils under lateral and angular misalignments. The more realistic geometrical arrangements are considered, and accurate approximations are made for efficient computations of the coupling coefficient of the radio-frequency coils used in implantable devices. A design procedure is proposed for coil designs, and a companion paper [1] discusses design techniques that are quite effective in stabilizing the link gain and bandwidth under misalignments with relatively high efficiency.

References

[1] D. C. Galbraith, M. Soma, and R. L. White, "A wide-band efficient inductive transdermal power and data link with coupling insensitive gain," *IEEE Trans. Biomed. Eng.*, this issue, pp. 265-275.

[2] W. H. Ko, S. P. Liang, and C. D. F. Fung, "Design of radio-frequency powered coils for implant instruments," *Med. Biol. Eng. Comput.*, vol. 15, pp. 634-640, Nov. 1977.

[3] F. C. Flack, E. D. James, and D. M. Schlapp, "Mutual inductance of air-cored coils: Effect on the design of radio-frequency coupled implants," *Med. Biol. Eng.*, vol. 9, pp. 79-85, Sept. 1971.

[4] E. S. Hochmair, "System optimization for improved accuracy in transcutaneous signal and power transmission," *IEEE Trans. Biomed. Eng.*, vol. BME-31, pp. 177-186, Feb. 1984.

[5] F. E. Terman, *Radio Engineers' Handbook*. New York: McGraw-Hill, 1943.

[6] S. Ramo, J. R. Whinnery, and T. Van Duzer, *Fields and Waves in Communication Electronics*. New York: Wiley, 1965.

[7] M. Soma, "Design and fabrication of an implantable multichannel neural stimulator," Tech. Rep. G 908-1, Stanford Electron. Lab., Stanford, CA, June 1980.

[8] F. W. Grover, *Inductance Calculations*. New York: Dover, 1973.

[9] *Collected Algorithms from ACM, 1*, Ass. Comput. Machin. New York: Ass. Comput. Machin., 1982, algorithms 55, 56, 149.

Mani Soma (S'74-M'80), for a photograph and biography, see this issue, p. 275.

Douglas C. Galbraith (S'77-S'79-S'80-M'85), for a photograph and biography, see this issue, p. 275.

Robert L. White (SM'68-F'77), for a photograph and biography, see this issue, p. 275.